



Research Article

CORRELATIONS FOR ESTIMATING CHANGE IN RESIDUAL OIL SATURATION DURING LOW SALINITY WATER FLOODING

Authors: David Alaigba*^{id}, Onaiwu Oduwa^{id}, Olalekan Olafuyi^{id}

To cite to this article: Alaigba, D., Oduwa, O., Olafuyi, O., (2021). Correlations for Estimating Change in Residual Oil Saturation During Low Salinity Water Flooding, *International Journal of Engineering and Innovative Research*, 3(2), p 101-114.

DOI: 10.47933/ijeir.838245

To link to this article: <https://dergipark.org.tr/tr/pub/ijeir/archive>



CORRELATIONS FOR ESTIMATING CHANGE IN RESIDUAL OIL SATURATION DURING LOW SALINITY WATER FLOODING

David Alaigba^{1*}, Onaiwu Oduwa¹, Olalekan Olafuyi¹

¹University of Benin, Faculty of Engineering, Petroleum Engineering, Benin-City, Nigeria.

*Corresponding Author: david.alaigba@gmail.com

(Received: 09.12.2020; Accepted: 17.02.2021)

<https://doi.org/10.47933/ijeir.838245>

ABSTRACT: Prior to embarking on a laboratory and subsequently pilot test for a potential improved oil recovery scheme in a green or brown field, it is important to have a sense of potential gains from the available options. This is usually done using correlations. Whereas there had been existing models for use in making these approximations, this work has developed a robust correlation for use in estimating the potential reduction in residual oil saturation post Optimized Salinity Water flooding (OPTSWF) (and consequently additional recovery) as a function of change in Interfacial tension (IFT), change in salinity, porosity, permeability, start residual oil saturation, and API gravity of the crude oil. This was done for a field in the Niger Delta. The model was tested against available data and showed good correlation with a correlation coefficient ranging from 99.36% to 99.89%. Also, the performance of the model was tested alongside that proposed by Tripathy et. al and in all cases, the model developed by this work performed better with lower RMS errors.

Keywords: Improved Oil Recovery, Optimized Salinity Water flooding, Niger Delta, Modeling.

1. INTRODUCTION

Water flooding is a secondary recovery scheme employed for optimal development of oilfields. This practice dates as far as the 1800s [1] Owing to its relative abundance, seawater with some treatment (for compatibility and to prevent formation damage) is one of the fluids employed for the injection.

The process typically entails the injection of water using dedicated injection wells for the following benefits:

- Voidage replacement leading to reservoir pressure maintenance
- Better volumetric sweep efficiencies
- Improved reserves, recoveries and project economics
- Effective management of produced water
- Energy security for coming generations
- Improved geomechanics or prevention of subsidence resulting from formation compaction (In cases where formations have high compressibilities)

Water flooding is a secondary recovery scheme which involves the injection of water into the reservoir to supplement the primary reservoir energy lost due to production by maintaining the reservoir pressure and also sweeping more oil towards the production wells. This has resulted

in improving recoveries up to 40-60% of the original oil in place [2]. Figure 1 depicts a typical water flooding scheme with surface and Sub-Surface processes.

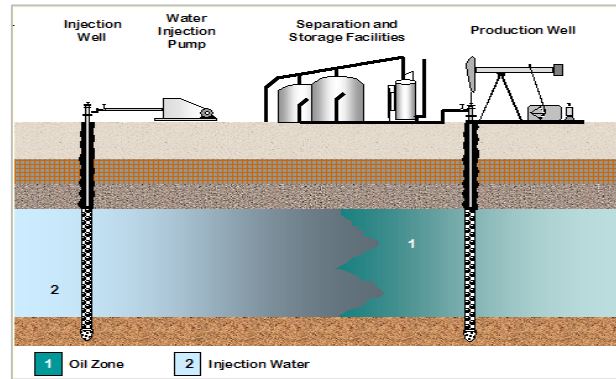


Figure 1. Waterflooding Schematic.

Low Salinity Waterflooding (LSWF), entails the use of diluted/Low Salinity Water (LSW) (500ppm-5000ppm of total dissolved solids) for injection instead of conventional sea water (35000ppm) or reservoir brine. Other names for LSWF in literature include; Smart Waterflooding, LoSal, Advanced Ion Management or Ion Tuning [3]. The author prefers to refer to the process as **Optimized Salinity Water Flooding (OPTSWF)**.

Among many attempts which have been made to model the effects of LSWF, the one proposed by Jerauld et al. [4] stands out. Their model which is based on the results of several core flood studies involving varying salinities of injection and connate brine. They observed that above and below a certain High Salinity (HS) and Low Salinity (LS) threshold, the injection brine salinity had no effect on oil recovery. The model assumes a linear dependence of relative permeability and capillary pressure on salinity between the thresholds. Equations 1 to 4 spell out the relationships. These equations have been successfully applied to history match LSWF experiments and field observations, [4, 5].

$$k_{rw} = \theta k_{rw}^{HS}(S^*) + (1 - \theta)k_{rw}^{LS}(S^*) \quad (1)$$

$$k_{row} = \theta k_{row}^{HS}(S^*) + (1 - \theta)k_{row}^{LS}(S^*) \quad (2)$$

$$P_{cow} = \theta P_{cow}^{HS}(S^*) + (1 - \theta)P_{cow}^{LS}(S^*) \quad (3)$$

$$\theta = \frac{S_{orw} - S_{orw}^{LS}}{S_{orw}^{HS} - S_{orw}^{LS}} \quad (4)$$

$$S^* = \frac{S_o - S_{orw}}{1 - S_{wr} - S_{orw}} \quad (5)$$

Tripathi and Mohanty, [6] in their attempt to model the LSWF process also adopted a linear dependence of relative permeability's, residual oil saturation and Corey's oil exponent on salt concentration. They then validated their model by using experimental data.

$$S_{or}(X_c) = S_{or}^{LS} + \frac{X_c - X_c^{LS}}{X_c^{LS} - X_c^{HS}} (S_{or}^{LS} - S_{or}^{HS}) \quad (6)$$

$$k_{rw}(X_c) = k_{rw}^{LS} + \frac{X_c - X_c^{LS}}{X_c^{LS} - X_c^{HS}} (k_{rw}^{LS} - k_{rw}^{HS}) \quad (7)$$

$$n_o(X_c) = n_o^{LS} + \frac{X_c - X_c^{LS}}{X_c^{LS} - X_c^{HS}} (n_o^{LS} - n_o^{HS}) \quad (8)$$

In applying the above models, Tripathi et al., [6] used Corey's equation [7] to model relative permeability and that of Skjaeveland [8] to generate capillary pressure curves. Relative permeabilities can also be derived using the Johnson-Bossler-Naumann (JBN) method or and the Jones and Roszelle (JR) technique from unsteady state flow experiments like core flooding, [9].

$$k_{rw} = k_{rw}^o (S_w^*)^{n_w} \quad (9)$$

$$k_{ro} = k_{ro}^o (1 - S_w^*)^{n_o} \quad (10)$$

$$S_w^* = \frac{S_w - S_{wr}}{1 - S_{wr} - S_{or}} \quad (11)$$

$$P_c = \frac{c_w}{\left(\frac{S_w - S_{wi}}{1 - S_{wi}}\right)^{a_w}} - \frac{c_o}{\left(\frac{1 - S_w - S_{or}}{1 - S_{or}}\right)^{a_o}} \quad (12)$$

Whereas many authors have attributed the observed LSE to an interplay of forces within the COBR system, both models do not account for the crude oil properties, pore structure parameters (porosity and permeability) and crude-brine interfacial tension, IFT.

More so, the current modeling approach of LSWF in literature is based on a linear dependence of rock and fluid properties on salinity, [6, 4]. The adoption of a linear relationship while easy to implement can lead to over simplification. It would be interesting to explore alternative and improved models and compare the obtained results with that currently in use.

Also, Al-Shalabi and Sepehrnoori [10] stressed that in modeling LSWF, emphasis should be placed on the oil composition so as to take into account possible reactions that could impact on the outcome of the LSWF scheme.

The objective of this research work is to develop robust correlations which incorporates parameters linked with the crude oil, water and rock properties for use in estimating the performance of OPSWF at the core scale. These correlations can then be used to screen potential OPSWF candidate fields before embarking on the expensive and time consuming laboratory experiments and pilot tests.

2. METHODOLOGY

This research adopted a mathematical modelling framework for use in obtaining robust correlations.

As emphasized by [11] the following parameters have been identified as impactful to the observed LSE effect in Niger Delta system;

- i. Change in IFT, ΔIFT

- ii. Change in Salinity, ΔSAL
- iii. PV of injected brine, PV_{inj}
- iv. Porosity of core, ϕ
- v. Core Permeability, K
- vi. Oil Saturation at start of OPTSWF S_{os} and
- vii. API gravity of crude oil. API

The formulation of the proposed equation is presented as:

$$\Delta S_{or} = C_0 + C_1(\Delta SAL)(\Delta IFT) + C_2 PV_{inj} + C_3 K^\phi + C_4 API^{S_{os}} \quad (13)$$

Where C_0, C_1, C_2, C_3 and C_4 are empirical constants derived from regressing OPTSWF experimental data.

$$\Delta S_{or} = C_0 + C_1 X_1 + C_2 X_2 + C_3 X_3 + C_4 X_4 \quad (14)$$

Where $X_1 = (\Delta SAL)(\Delta IFT), X_2 = PV_{inj}, X_3 = K^\phi, X_4 = API^{S_{os}}$

Discretizing,

$$\Delta S_{ori} = C_0 X_{0i} + C_1 X_{1i} + C_2 X_{2i} + C_3 X_{3i} + C_4 X_{4i} \quad (15)$$

For a data set of $i = 1$ to n , we have an n by 5 matrix for ΔS_{ori} .

Let X equal to the $n \times 5$ matrix containing X_{01} to X_{4n} .

$$X = \begin{bmatrix} X_{01} & X_{11} & X_{12} & X_{13} & X_{14} \\ X_{02} & X_{21} & X_{22} & X_{23} & X_{24} \\ X_{03} & X_{31} & X_{32} & X_{33} & X_{34} \\ \dots & \dots & \dots & \dots & \dots \\ X_{0n} & X_{n1} & X_{n2} & X_{n3} & X_{n4} \end{bmatrix}$$

Let C be equal to a vector containing C_0, C_1, C_2, C_3 and C_4

$$C = \begin{bmatrix} C_0 \\ C_1 \\ C_2 \\ C_3 \\ C_4 \end{bmatrix}$$

Let y be the vector of experimental observations of ΔS_{ori} ($i = 1$ to n).

$$y = \begin{bmatrix} \Delta S_{or1} \\ \Delta S_{or2} \\ \Delta S_{or3} \\ \dots \\ \Delta S_{orn} \end{bmatrix}$$

To solve for the constants C_0, C_1, C_2, C_3 and C_4 , we can make use of the normal equation [12] as follows;

$$C = (X^T X)^{-1} \cdot (X^T y) \quad (16)$$

2.1. Data for Study

The data for study were sourced from [11] and is presented in Table 1 and **Error! Reference source not found..** It can be observed that $n = 16$.

Table 1. Raw Experimental Data.

S/NO	SALT	ΔIFT	ΔSAL	PVINJ	K	PHI	API	SOS	ΔSOR	DRF
1	NACL	62.60	5000.00	1.00	298.10	0.20	26.25	0.51	0.08	0.09
2	NACL	60.50	2500.00	0.50	298.10	0.20	26.25	0.51	0.02	0.03
3	NACL	58.50	1000.00	0.50	298.10	0.20	26.25	0.51	0.04	0.04
4	NACL	55.30	625.00	0.38	298.10	0.20	26.25	0.51	0.01	0.01
5	K2SO4	55.30	5000.00	1.65	274.00	0.23	26.25	0.63	0.10	0.10
6	K2SO4	54.60	2500.00	1.05	274.00	0.23	26.25	0.63	0.04	0.04
7	K2SO4	54.50	1000.00	0.60	274.00	0.23	26.25	0.63	0.01	0.01
8	K2SO4	52.60	625.00	0.45	274.00	0.23	26.25	0.63	0.01	0.01
9	CACL2	51.90	5000.00	1.77	268.00	0.22	26.25	0.62	0.19	0.21
10	CACL2	46.50	2500.00	1.13	268.00	0.22	26.25	0.62	0.04	0.05
11	CACL2	44.80	1000.00	0.65	268.00	0.22	26.25	0.62	0.03	0.03
12	CACL2	43.60	625.00	0.48	268.00	0.22	26.25	0.62	0.01	0.02
13	MGSO4	55.50	5000.00	0.95	293.00	0.20	26.25	0.70	0.18	0.19
14	MGSO4	53.20	2500.00	1.07	293.00	0.20	26.25	0.70	0.10	0.10
15	MGSO4	51.90	1000.00	0.71	293.00	0.20	26.25	0.70	0.02	0.02
16	MGSO4	48.90	625.00	0.12	293.00	0.20	26.25	0.70	0.00	0.00

Table 2. Refined experimental data ready for modeling.

i	X0	X1=DIFT*DSAL/100000	X2=PVINJ	X3=K^PHI	X4=API^SOS	Y=DSOR_EXP
1	1	3.13	1.00	3.13	5.25	0.08
2	1	1.51	0.50	3.13	5.25	0.02
3	1	0.59	0.50	3.13	5.25	0.04
4	1	0.35	0.38	3.13	5.25	0.01
5	1	2.77	1.65	3.64	7.78	0.10
6	1	1.37	1.05	3.64	7.78	0.04
7	1	0.55	0.60	3.64	7.78	0.01
8	1	0.33	0.45	3.64	7.78	0.01
9	1	2.60	1.77	3.42	7.68	0.19
10	1	1.16	1.13	3.42	7.68	0.04
11	1	0.45	0.65	3.42	7.68	0.03
12	1	0.27	0.48	3.42	7.68	0.01
13	1	2.78	0.95	3.11	9.80	0.18
14	1	1.33	1.07	3.11	9.80	0.10
15	1	0.52	0.71	3.11	9.80	0.02
16	1	0.31	0.12	3.11	9.80	0.00

3. RESULTS/ DISCUSSIONS

3.1. Correlation for Four Brines - NACL, K2SO4, CACL2, MGSO4

The normal equation 16 was applied to the data set presented in Table 2 to obtain the correlation coefficients in **Error! Reference source not found.** Equation 17 is obtained by substituting these parameters in equation 13. Figure 2 shows a comparison of the model calculated and experimentally derived change in oil saturation and the match is very good with the trend closely followed. The error margin is 0.64%.

Table 3. Correlation Parameters for All Salts.

DSOR_ALL	
c0	0.110045
c1	0.027029
c2	0.061203
c3	-0.05858
c4	0.007361

$$\Delta S_{orALL} = 0.110045 + 0.027029(\Delta SAL)(\Delta IFT) + 0.061203PV_{inj} - 0.05858K^{\phi} + 0.007361API^{S_{os}} \tag{17}$$

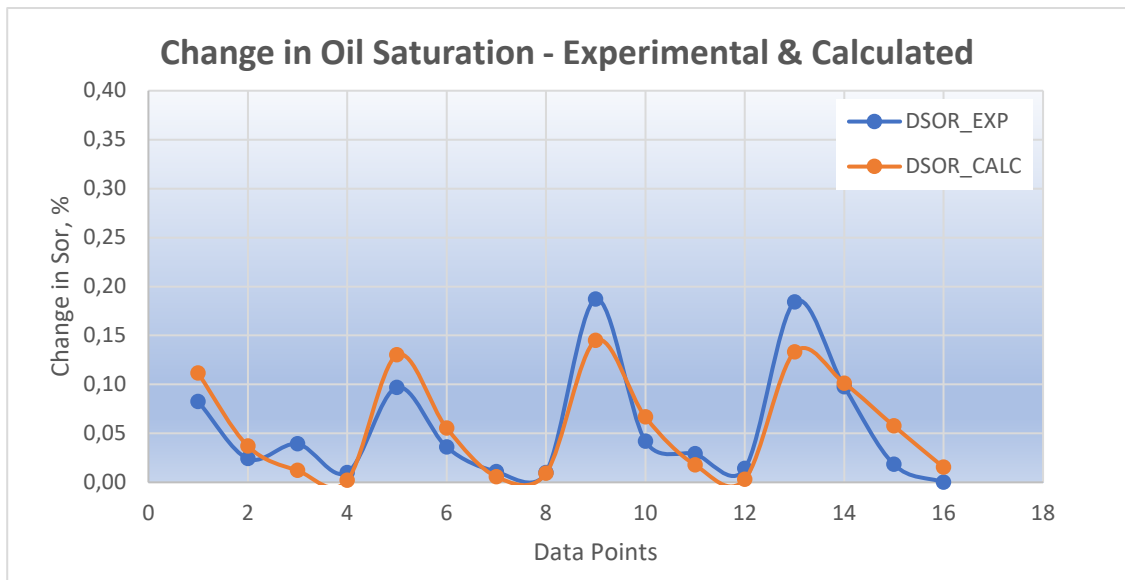


Figure 2. Experimental DSOR vs Model DSOR – All Salts.

3.2. Correlation for NACL

The normal equation 16 was applied to the data set presented in Table 4 to obtain the correlation coefficients in Table 5. Equation 18 is obtained by substituting these parameters in equation 13. Figure 3 and Table 6 show a comparison of the model calculated and experimentally derived change in oil saturation and the match is very good with the trend closely followed. The error margin is 0.25%.

Table 4. NACL Experimental Data.

SAL, PPM	X0	X1=DIFT*DSAL/100000	X2=PVINJ	X3=K^PHI	X4=API^SOS	Y = DSOR_EXP
5000	1	3.13	1.00	3.13	5.25	8%
2500	1	1.51	0.50	3.13	5.25	2%
1250	1	0.59	0.50	3.13	5.25	4%
625	1	0.35	0.38	3.13	5.25	1%

Table 5: Correlation Parameters for NaCl.

DSOR_NACL	
c0	-0.00127
c1	-0.01869
c2	0.188801
c3	-0.00398
c4	-0.00667

$$\Delta S_{orNACL} = -0.00127 - 0.01869(\Delta SAL)(\Delta IFT) + 0.188801PV_{inj} - 0.00398K^{\phi} - 0.00667API^{S_{os}} \tag{18}$$

Table 6. Experimental Vs Model Calculated DSOR – NACL

DSAL	DSOR_EXP	DSOR_CALC
5000	8%	8%
2500	2%	2%
1000	4%	3%
625	1%	2%

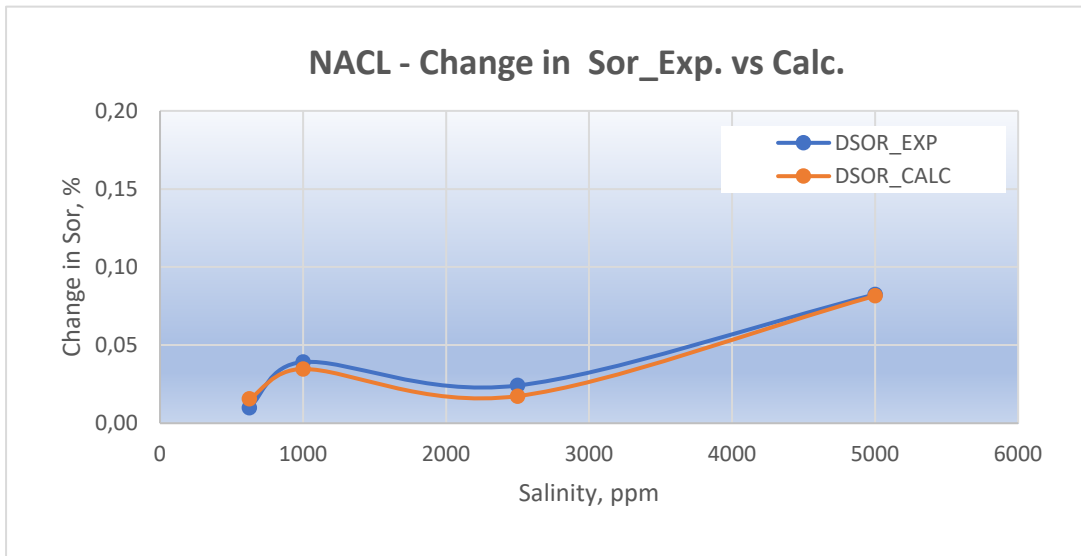


Figure 3. Experimental DSOR Vs Model DSOR – NACL.

3.3. Correlation for K2SO4

The normal equation 16 was applied to the data set presented in Table 7 to obtain the correlation coefficients in Table 8. Equation 19 is obtained by substituting these parameters in equation 13. Figure 4 and Table 9 show a comparison of the model calculated and experimentally derived change in oil saturation and the match is very good with the trend closely followed. The error margin is 0.11%.

TABLE 7. K2SO4 Experimental Data.

S/NO	X0	X1=DIFT*DSAL/100000	X2=PVINJ	X3=K^PHI	X4=API^SOS	Y = DSOR_EXP
5000	1	2.77	1.65	3.64	7.78	10%
2500	1	1.37	1.05	3.64	7.78	4%
1250	1	0.55	0.60	3.64	7.78	1%
625	1	0.33	0.45	3.64	7.78	1%

Table 8. Correlation Parameters for K2SO4.

DSOR_K2SO4	
c0	0.000326
c1	0.086268
c2	-0.09883
c3	0.001187
c4	0.002537

$$\Delta S_{orK_2SO_4} = 0.000326 - 0.086268(\Delta SAL)(\Delta IFT) - 0.09883PV_{inj} + 0.001187K^\phi + 0.02537API^{S_{os}} \quad (19)$$

Table 9. Experimental Vs Model Calculated DSOR – K2SO4.

DSAL	DSOR_EXP	DSOR_CALC
5000	10%	10%
2500	4%	4%
1000	1%	1%
625	1%	1%

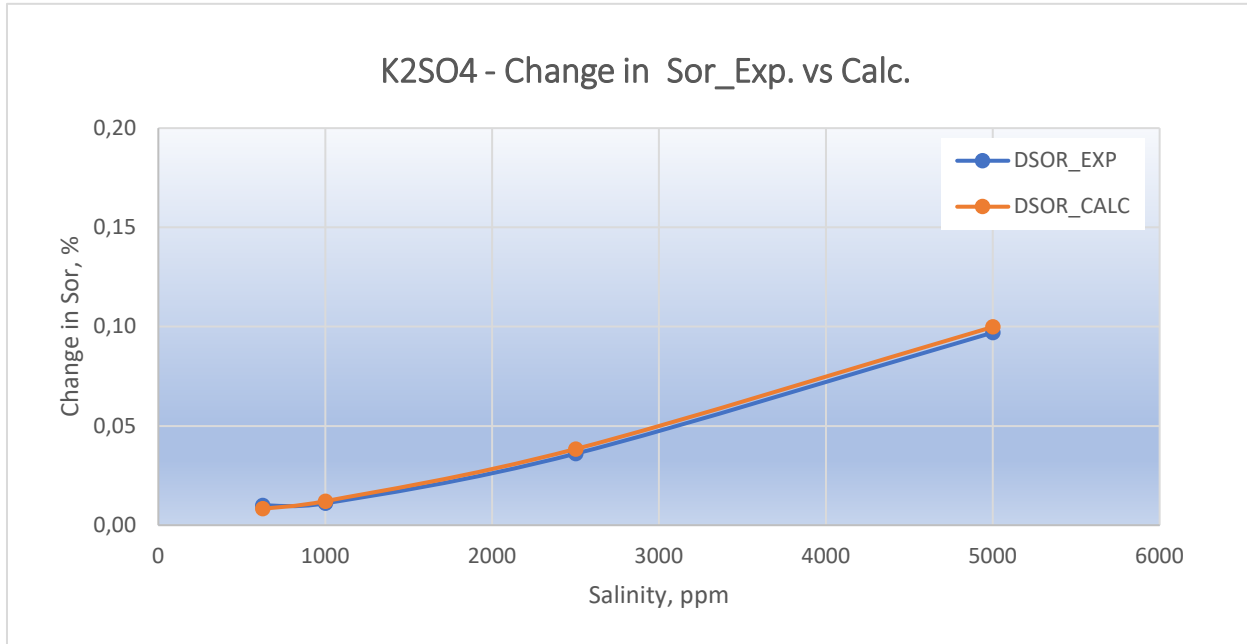


Figure 4. Experimental DSOR vs Model DSOR – K2SO4.

3.4. Correlation for CACL2

The normal equation 16 was applied to the data set presented in Table 10 to obtain the correlation coefficients in Table 11. Equation 20 is obtained by substituting these parameters in equation 13. Figure 5 and Table 12 show a comparison of the model calculated and

experimentally derived change in oil saturation and the match is very good with the trend closely followed. The error margin is 0.37%.

Table 10. CACL2 Experimental Data.

S/NO	X0	X1=DIFT*DSAL/100000	X2=PVINJ	X3=K^PHI	X4=API^SOS	Y = DSOR_EXP
5000	1	2.60	1.77	3.42	7.68	19%
2500	1	1.16	1.13	3.42	7.68	4%
1250	1	0.45	0.65	3.42	7.68	3%
625	1	0.27	0.48	3.42	7.68	1%

Table 11. Correlation Parameters for CACL2

DSOR_CACL2	
c0	0.001097
c1	0.204884
c2	-0.23879
c3	0.003751
c4	0.008423

$$\Delta S_{orCACL_2} = 0.001097 + 0.204884(\Delta SAL)(\Delta IFT) - 0.23879PV_{inj} + 0.003751K^\phi + 0.008423API^{S_{os}} \tag{20}$$

Table 12. Experimental vs Model Calculated DSOR – CACL2.

DSAL	DSOR_EXP	DSOR_CALC
5000	19%	19%
2500	4%	5%
1000	3%	2%
625	1%	2%

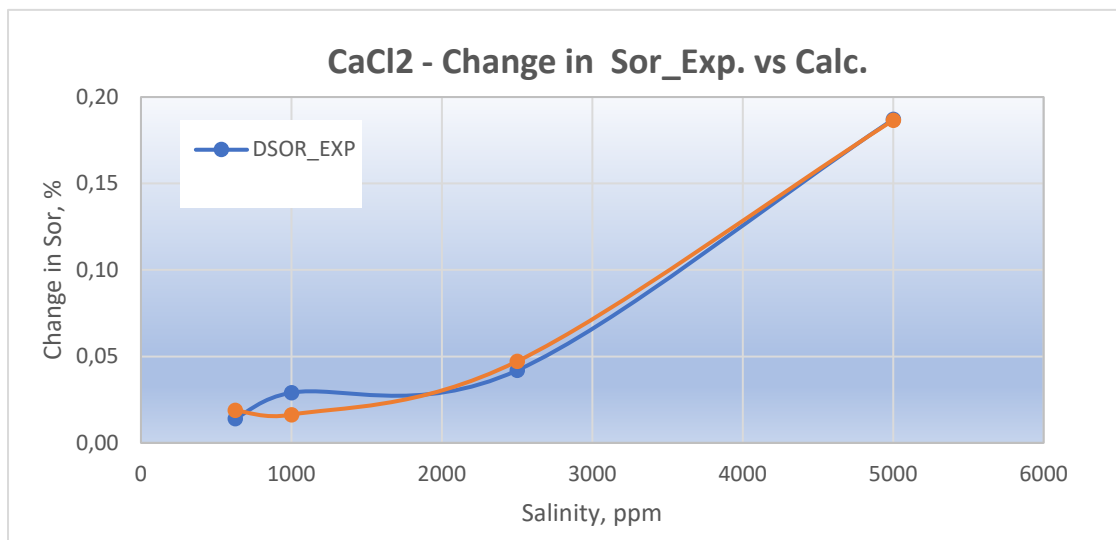


Figure 5: Experimental DSOR vs Model DSOR – CACL2.

3.5. Correlation for MGSO4

The normal equation 16 was applied to the data set presented in Table 13 to obtain the correlation coefficients in Table 14. Equation 21 is obtained by substituting these parameters in equation 13. Figure 6 and Table 15 show a comparison of the model calculated and experimentally derived change in oil saturation and the match is very good with the trend closely followed. The error margin is 0.37%.

Table 13. MGSO4 Experimental Data.

S/NO	X0	X1=DIFT*DSAL/100000	X2=PVINJ	X3=K^PHI	X4=API^SOS	Y = DSOR_EXP
5000	1	2.78	0.95	3.11	9.80	18%
2500	1	1.33	1.07	3.11	9.80	10%
1250	1	0.52	0.71	3.11	9.80	2%
625	1	0.31	0.12	3.11	9.80	0%

Table 14. Correlation Parameters for MGSO4.

DSOR_MGSO4	
c0	-0.00026
c1	0.064583
c2	0.031848
c3	-0.0008
c4	-0.00252

$$S_{orMGSO_4} = -0.00026 + 0.064583(\Delta SAL)(\Delta IFT) + 0.031848PV_{inj} - 0.0008K^{\phi} - 0.00252API^{S_{os}} \quad (21)$$

Table 15. Experimental vs Model Calculated DSOR – MGSO4.

DSAL	DSOR_EXP	DSOR_CALC
5000	18%	18%
2500	10%	9%
1000	2%	3%
625	0%	0%

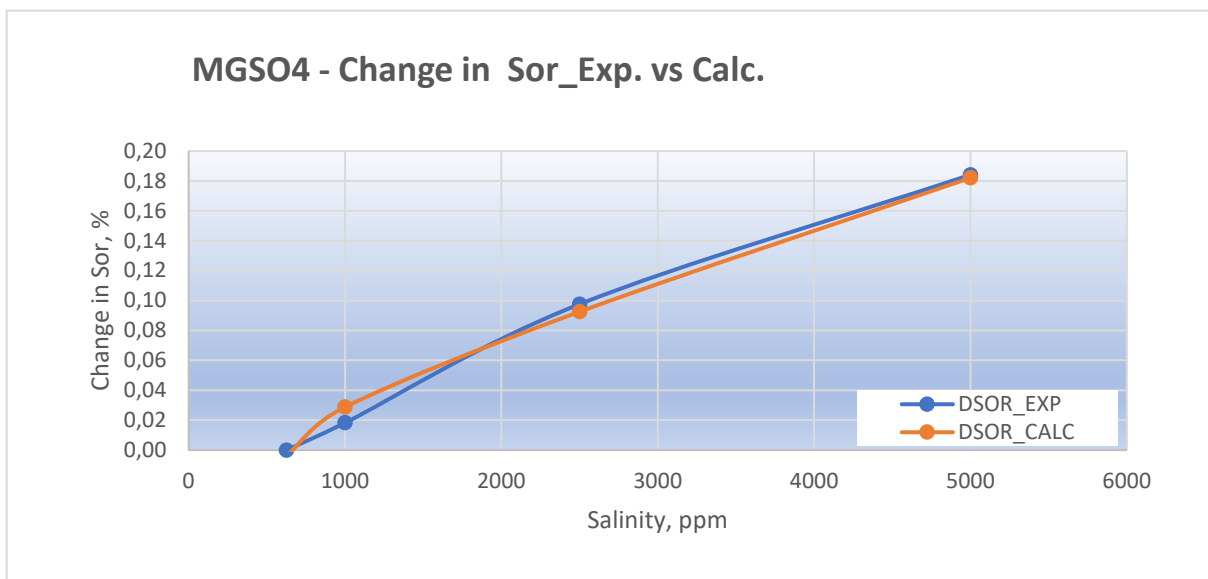


Figure 6. Experimental DSOR vs Model DSOR – MGSO4.

3.6. Derived Model vs Tripathy and Mohanty's Model

The derived model for the four salts was compared with an existing one [6] and the results for the four salts are presented in Figure 7, Figure 8, Figure 9 and Figure 10. It is to be noted that the model derived by this work shows consistently better match with the observed experimental results. Table 16 summarizes the error comparison between the model from this work and that from [6].

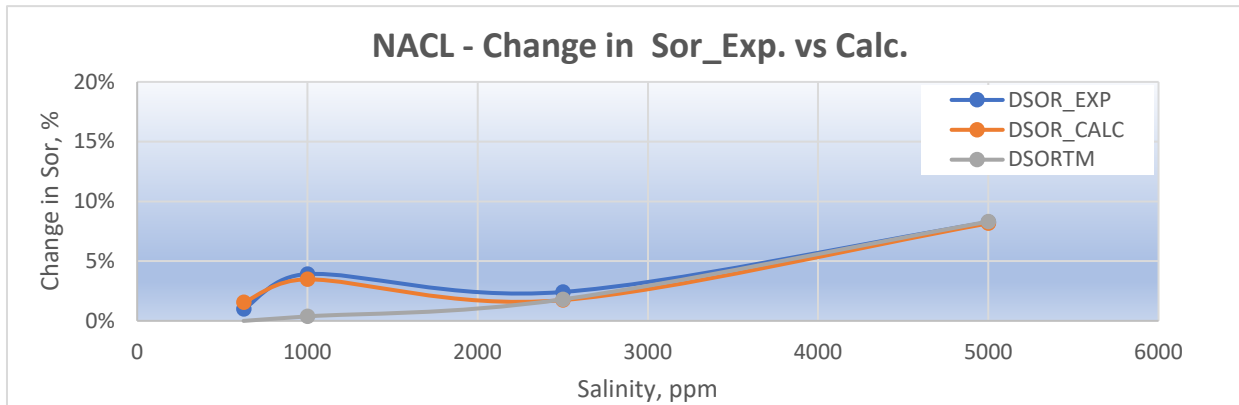


Figure 7. Comparison between Derived Model and Tripathy and Mohanty's – NaCl.

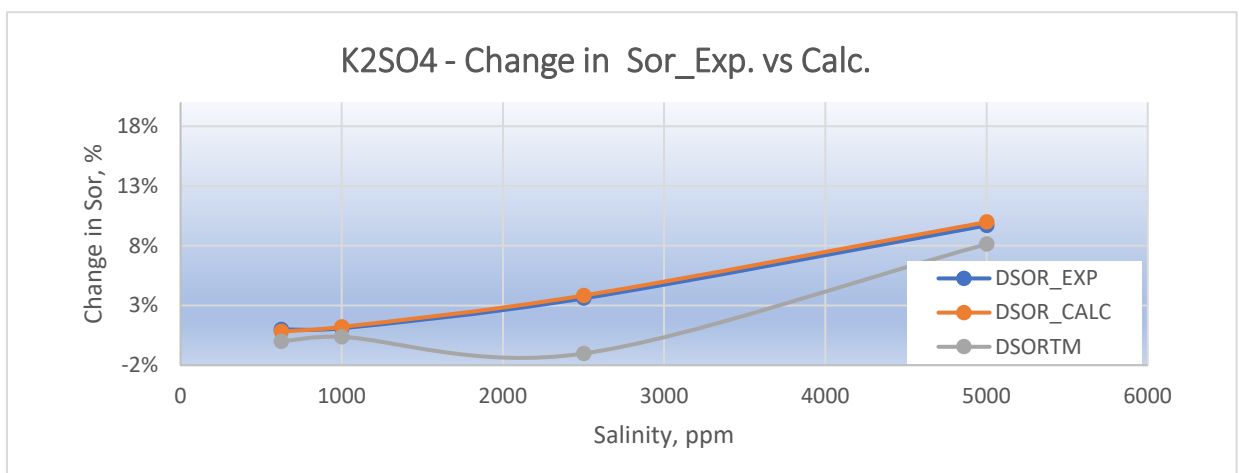


Figure 8. Comparison between Derived Model and Tripathy and Mohanty's – K2SO4.

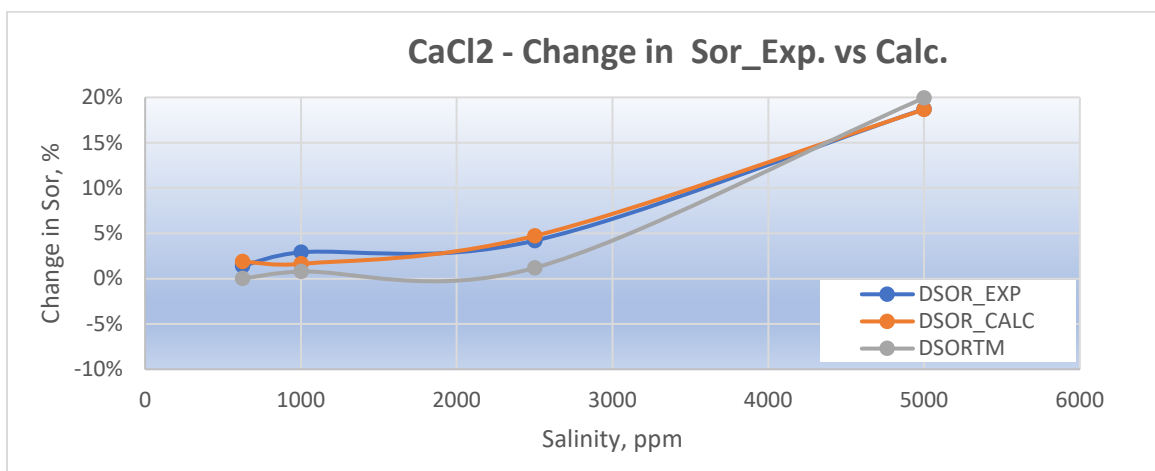


Figure 9. Comparison Between Derived Model and Tripathy and Mohanty's – CaCl2.

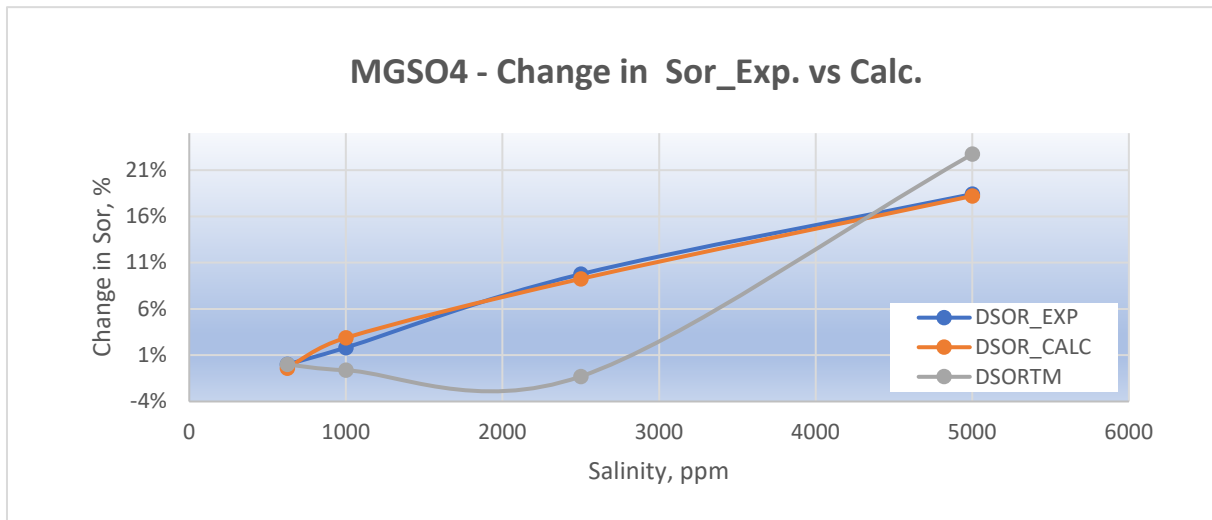


Figure 10. Comparison between Derived Model and Tripathi and Mohanty's – MGSO4.

Table 16: Error Comparison between This Model and Tripathi and Mahanty's Model.

BRINE	ERROR_THIS MODEL	ERROR_T&M
NACL	0.25%	0.93%
K2SO4	0.11%	5.23%
CACL2	0.37%	1.03%
MGSO4	0.31%	3.03%

4. CONCLUSION and RECOMMENDATIONS

In conclusion, robust models which have integrated both rock and fluid properties have been developed for the estimation of potential reduction in residual oil saturation post-OPSWF for four salts and these have been tested with very good matches with laboratory data. The performance of the models were also compared with a previously existing model and in all cases, the models developed in this work produced better results with lower error margins when compared with the previously existing model. Areas of applications would include screening of IOR candidates to estimate potential gains by implementing the OPSWF scheme and benchmarking laboratory results. In contrast to existing models, the models developed in this work takes into account the brine, rock and crude oil properties.

The following areas can be taken up for further studies

1. Integrate additional experiments and update model
2. Test developed model on data from other authors across globe

ACKNOWLEDGEMENTS

The authors would like to appreciate the Department of Petroleum Resources and Platform Petroleum Nigeria Limited for providing the research materials used in this study. The authors would also like to thank the Petroleum Engineering Laboratories at: University of Benin, University of Ibadan and Covenant University, Ota.

REFERENCES

- [1] I. G. B. J. Satter A, Practical Enhanced reservoir Engineering, Tulsa: PennWell, 2008.
- [2] BP, "Statistical Review of World Energy," London, 2020.
- [3] H. M. S. B. S. H. W.-B. Bartels, "Literature review of low salinity waterflooding from a length and time scale perspective," Fuel, vol. 236, no. 236, pp. 338-353, 2019.
- [4] Gary R. Jerauld, C.Y. Lin, Kevin J. Webb and Jim C. Seccombe, "Modeling Low-Salinity Waterflooding. SPE-102239-PA," in 2006 SPE Annual Technical Conference and Exhibition, an Antonio, Texas, 2008.
- [5] Mohammad-Javad Shojaei, Mohammad Hossein Ghazanfari and Moshen Masihi, "Relative Permeability and Capillary Pressure Curves for Low Salinity Waterflooding in Sandstone Rocks," Journal of Natural Gas Science and Engineering, vol. 25, pp. 30-38, 2015.
- [6] Tripathi, I., Mohanty, K., "Instability due to wettability alteration in displacements through porous media," Chem. Eng. Sci., vol. 63, pp. 5366-5374, 2008.
- [7] Delshad, M., Pope, G.A., "Comparison of the three-phase oil relative permeability models," Transp. Porous Media, vol. 4, pp. 59-83, 1989.
- [8] Skjaeveland, S., Siqveland, L., Kjosavik, A., Hammervold, W., Virnovsky, G., "Capillary pressure correlation for mixed-wet reservoirs," SPE Journal Paper, vol. 3, no. 01, 2000.
- [9] Richard L. Christiansen, James S. Kalbus, Susan M. Howarth, "Evaluation of Methods for Measuring Relative Permeability of Anhydrite from the Salado Formation: Sensitivity Analysis and Data Reduction," Sandia National Laboratories, Albuquerque, New Mexico, 1997.
- [10] Emad W. Al-Shalabi, Kamy Sepehrnoori, "A comprehensive review of low salinity/engineered water injections," Journal of Petroleum Science and Engineering, vol. 139, p. 137–161, 2015.
- [11] Alaigba David, Oduwa Onaiwu, Ohenhen Ikponmwosa, Olafuyi Olalekan, "Optimized Salinity Water Flooding as an Improved Oil Recovery IOR Scheme in the Niger Delta," in SPE Nigeria Annual International Conference and Exhibition, 11-13 August, Virtual, Lagos, Nigeria, 2020.
- [12] N. Springer New York, "Normal Equations In: The Concise Encyclopedia of Statistics Springer, New York, NY.," New York, 2008.
- [13] C. Myers, Intelligent Buildings: A Guide for Facility Managers, Newyork: Upword Publishing, 1996.
- [14] K. G. Shankar , "Control of Boiler Operation using PLC – SCADA," in Proceedings of the International MultiConference of Engineers and Computer Scientists 2008, Hong Kong, 2008.
- [15] J. Figueiredo and J. da Costab, "A SCADA system for energy management in intelligent buildings," Energy and Buildings, pp. 85-98, 2012.
- [16] Z. Zheng and A. N. Reddy, "Towards Improving Data Validity of Cyber-Physical Systems through Path Redundancy," in CPSS '17 Proceedings of the 3rd ACM Workshop on Cyber-Physical System Security, Abu Dhabi, 2017.
- [17] R. Bayındır, O. Kaplan, C. Bayyığıt, Y. Sarıkaya and M. Hallaçlıoğlu, "PLC ve SCADA kullanılarak bir endüstriyel sistemin otomasyonu," Erciyes Üniversitesi Fen Bilimleri Enstitüsü Dergisi, pp. 107-115, 2011.
- [18] İ. Kırık and N. Özdemir, "PLC kontrollü sürekli tahrikli sürtünme kaynak makinesinin tasarım ve imalatı," in International Conference on Welding Technologies and Exhibition , Ankara, 2012.

NOMENCLATURE

θ -	Interpolation Parameter
r -	Pore Radius
q -	Flow Rate of Injection
k -	Absolute Permeability
PV_{inj} -	PV Brine Injected
API -	API Gravity of Crude Oil
SWCTT -	Single Well Chemical Tracer Test
PV -	Pore Volume
PPM -	Parts per Million
OPTSWF -	Optimized Salinity Water flooding
NPV -	Net Present Value
LSWF -	Low Salinity Water Flooding

IRR -	Internal Rate of Return
IFT -	Interfacial Tension
COBR -	Crude Oil-Brine-Rock
CBRS -	Crude Oil-Brine-Rock System
CBR -	Crude-Brine-Rock
ΔSAL -	Change in Salinity
ΔIFT -	Change in IFT
\emptyset -	Porosity
σ_{ow} -	Oil-Water Interfacial Tension, IFT
μ_w -	Water viscosity
μ_o -	Oil Viscosity
n_w -	Corey's oil Parameter
n_o^{LS} -	Corey's oil Parameter at LS Condition
n_o^{HS} -	Corey's oil Parameter at HS Condition
$n_o(X_c)$ -	Corey's Oil Parameter
n_o -	Corey's oil Parameter
k_{rw}^{LS} -	Relative Permeability to Water at LS Condition
k_{rw}^{HS} -	Relative Permeability to Water at HS Condition
$k_{rw}(X_c)$ -	Relative Permeability to Water as a Function of Salinity
k_{rw} -	Relative Permeability to Water
k_{ro} -	Relative Permeability to Oil
c_w -	Water Compressibility
c_o -	Oil Compressibility
X_c^{LS} -	Brine Salinity at LS Condition
X_c^{HS} -	Brine Salinity at HS Condition
X_c -	Brine Salinity
S_{wr} -	Residual water saturation
S_{wi} -	Initial Water Saturation
S_w^* -	Average water saturation
S_{os} -	Oil saturation at start of OPTSWF
S_{or}^{LS} -	Residual Oil Saturation Post-LS Flooding
S_{or}^{HS} -	Residual Oil Saturation Post-HS Flooding
$S_{or}(X_c)$ -	Oil Saturation as a Function of Salinity
S_{or} -	Residual Oil Saturation
S_o -	Oil Saturation
P_c -	Capillary Pressure